Transverse Location of the Fluorescent Probe 1,6-Diphenyl-1,3,5-hexatriene in Model Lipid Bilayer Membrane Systems by Resonance Excitation Energy Transfer†

Lesley Davenport,*,‡ Robert E. Dale,§ Roger H. Bisby,‡ and Robert B. Cundall‡

Department of Biochemistry, University of Salford, Salford M5 4WT, U.K., and Paterson Laboratories, Christie Hospital and Holt Radium Institute, Manchester M20 9BX, U.K.

Received August 15, 1984; Revised Manuscript Received February 20, 1985

ABSTRACT: A fluorescent phospholipid derivative, the fluoresceinthiocarbamyl adduct of a natural phosphatidylethanolamine, has been synthesized and incorporated into sonicated single-bilayer vesicles of egg lecithin and dipalmitoyllecithin. The surface location of this probe has been confirmed by using extrinsic fluorescence quenching studies together with steady-state emission anisotropy measurements. Electronic excitation energy transfer between 1,6-diphenyl-1,3,5-hexatriene incorporated within the hydrophobic core of the bilayer and the novel derivative has been investigated to estimate the depth within the bilayer at which the former is located. Efficiencies have been measured for two different phospholipids, egg lecithin and dipalmitoyllecithin, in the latter case both above and below the phospholipid phase transition, with and without added cholesterol. The observed dependence of the transfer efficiency on the acceptor concentration was compared with that calculated according to Förster theory applied to random two-dimensional distributions of donor and acceptor molecules in parallel planes for various interplanar separations, taking into account orientational effects. The Förster R_0 of about 45 Å for this donor–acceptor pair is particularly well suited to such studies since it is of the order of the width of the bilayer. The experiments showed that energy-transfer spectroscopy can provide useful quantitative information as to the transverse location of diphenylhexatriene in homogeneous phospholipid bilayers and may also reflect lateral partitioning of donor or of both donor and acceptor into different phases in systems exhibiting phase separations.

In recent years, long-range nonradiative singlet–singlet (Förster) resonance excitation energy transfer (FRET)[1] has become widely used as a "spectroscopic ruler" to determine intramolecular separations and conformational dynamics of mainly biological macromolecules and organized assemblies in the 10–100-Å range (Fairclough & Cantor, 1978; Stryer, 1978).

Fluorescence quenching and resonance energy transfer methods have been used to investigate the distribution of fluorophores in both the lateral [e.g., see Fung & Stryer (1978), Wharton et al. (1980), and Holowka & Baird (1983a)] and transverse planes of the lipid bilayer. In the latter application, a series of *n*-(9-anthroyloxy) fatty acids synthesized to position the fluorophore at graded depths within the lipid bilayer has been examined (Haigh et al., 1979; Eisinger & Flores, 1983). Transfer from an intrinsic fluorescent tryptophanyl residue of cytochrome b_5 to extrinsic acceptor molecules positioned in the polar head-group region of phospholipid vesicles has been used to locate the depth of the residue in the bilayer (Fleming et al., 1979). The location of different fluorescently labeled domains of immunoglobulin E bound to receptors on rat basophilic leukemia cell plasma membranes with respect to surface-bound energy-transfer acceptors has also been determined (Holowka & Baird, 1983b) and the distribution of fluorescently-labeled concanavalin A on the surfaces of normal and transformed fibroblasts investigated by energy transfer (Dale et al., 1981). Energy transfer in the rapid diffusion limit from a Tb^{3+} chelate entrapped inside vesicles to an eosinphosphatidylethanolamine derivative incorporated into the vesicle bilayer has allowed a determination of their distance of closest approach (Thomas et al., 1978).

Considerable interest has also been generated in the role played in the regulation of membrane-mediated events by the physical state of membrane lipids, i.e., by their structure and dynamics, within the context of the fluid mosaic membrane hypothesis (Singer & Nicolson, 1972).

1,6-Diphenyl-1,3,5-hexatriene (DPH) is perhaps the most widely used of all so-called "microviscosity" probes in membrane biochemistry for assessing fluidity and structural parameters of the fatty acyl chain region of both natural and synthetic membranes via the depolarization of its fluorescence (Shinitzky & Barenholz, 1978; Shinitzky & Yuli, 1982; Zannoni et al., 1983). Although DPH is known to penetrate the hydrophobic core of the bilayer and preferentially orient perpendicularly to its plane (Andrich & Vanderkooi, 1976), the exact depth or range of depths at which this probe lies within the bilayer structure is still unknown. It has been reported that the packing of the phospholipid molecules and the rotational motions of their fatty acyl chains differ with phospholipid type and along the carbon chain length (Seelig & Seelig, 1980). Furthermore, perturbation of this architecture results from the presence of cholesterol, antibiotics, and other fused ring systems in the bilayer (Barrett-Bee et al., 1972; Gent & Pretegard, 1974; Hartmann et al., 1978; Ohki

† This research was supported by the Science Research Council, the Cancer Research Campaign, and the Medical Research Council.

* Correspondence should be addressed to this author at the Department of Chemistry, Brooklyn College of the City University of New York, Brooklyn, NY 11210.

‡ University of Salford.

§ Christie Hospital and Holt Radium Institute.

[1] Abbreviations: FRET, Förster resonance energy transfer; DPH, 1,6-diphenyl-1,3,5-hexatriene; F-PE, fluoresceinthiocarbamylphosphatidylethanolamine; EL, egg lecithin; DPL, dipalmitoyl-DL-α-lecithin; FITC, fluorescein isothiocyanate; TLC, thin-layer chromatography; PE, phosphatidylethanolamine; THF, tetrahydrofuran; EM, electron microscopy; T_c, phospholipid bilayer gel/liquid-crystalline phase transition temperature; Tris·HCl, tris(hydroxymethyl)aminomethane hydrochloride.

0006-2960/85/0424-4097$01.50/0

et al., 1979). A transverse "fluidity gradient" has also been deduced from fluorescence depolarization measurements on the series of *n*-(9-anthroyloxy) fatty acids already mentioned (Tilley et al., 1979). Thus, the transverse location of DPH is an important parameter to be identified when attempting to interpret the structural and dynamic characteristics both of model phospholipid membrane systems and of natural membranes probed in this way.

Advantage has been taken of the reactivity of the primary amino group of phosphatidylethanolamine to synthesize a fluorescent phospholipid derivative, the fluoresceinthiocarbamyl adduct of phosphatidylethanolamine (F-PE), for use as an energy-transfer acceptor. Minimization of membrane perturbation by the use of a fluorescent derivative of a natural phospholipid analogue is an attractive advantage.

In the following, attempts to determine the transverse location of DPH in model membrane systems via estimates of the separation between the planes containing the fluorescent acceptor moiety of F-PE located at the surface of the bilayer and the donor DPH buried in its hydrophobic interior from FRET efficiencies are reported and interpreted, taking into account orientational effects. Model lipid membranes of egg lecithin (EL) and dipalmitoyllecithin (DPL), the latter above and below its phase transition temperature T_c, in both the absence and presence of cholesterol, were examined. These membranes provide a wide range of relative reorientational freedom of the donor. Use is made of an equation developed from Förster theory (Förster, 1949) for energy transfer from donors situated outside a random planar distribution of acceptor which includes orientational effects and which differs from those previously reported in the literature (Wolber & Hudson, 1979; Koppel et al., 1979; Haigh et al., 1979; Dewey & Hammes, 1980).

Theory

A quantitative interpretation of the FRET measurements reported in the present contribution for the anisotropic systems examined not only requires solution of the problem of Förster long-range transfer between isolated donors situated at some distance from an array of acceptors randomly distributed over a two-dimensional surface but also should take into account their relative orientations. The simplest case, that of a planar array with all donor (D) and acceptor (A) pairs exhibiting an identical orientational dependence (specifically, with orientation factors taking their dynamic random average value, $\langle\kappa^2\rangle = {}^2/_3$), has previously been dealt with exactly (Wolber & Hudson, 1979). In the following, this case will be rederived in a form particularly suitable for taking into account orientational effects, which will then be included in the dynamic limit.

The spatial geometry relevant to the above model transfer system is shown in Figure 1. Following the usual treatment (Förster, 1949; Tweet et al., 1964; Wolber & Hudson, 1979), the decay of the donor emission, $\bar{p}(t)$, averaged over all possible statistical arrangements of N acceptors over the surface of the disk of area $A_d = \pi r_d^2$, is given by

$$\bar{p}(t) = e^{-t/\tau}\prod^{N}\int_{R=a}^{(a^2+r_d^2)^{1/2}} \exp[-(t/\tau)(R_0/R)^6]\omega(R)\,dR = \exp(-t/\tau)[J(t)]^N \quad (1)$$

where R_0, the Förster critical transfer separation, is given by

$$R_0^6 = \frac{9(\ln 10)\Phi\kappa^2}{128\pi^5 N' n^4}\left[\frac{\int_0^\infty \epsilon_A(\lambda)F_D(\lambda)\lambda^4\,d\lambda}{\int_0^\infty F_D(\lambda)\,d\lambda}\right] \quad (2)$$

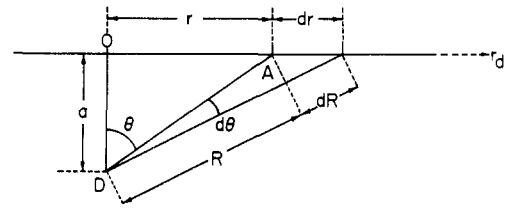

FIGURE 1: Spatial geometry of model transfer system represented as a cross section through the acceptor-containing plane envisaged as a disk of radius r_d containing N randomly distributed acceptors and a donor (D) situated at a distance a from the center (0) of the disk along a normal to its plane. The angular and spatial relationships of a particular acceptor (A) to the donor are depicted and related by $R = a\sec\theta$, $r = a\tan\theta$, and $dr = a\sec^2\theta\,d\theta$.

in which Φ is the donor quantum yield in the absence of acceptor, κ^2 the orientation factor for dipole–dipole coupling, $\epsilon_A(\lambda)$ the molar absorbance of the acceptor at wavelength λ, $F_D(\lambda)$ the fluorescence intensity of the donor per unit wavelength interval, N' Avogadro's number per millimole, and n the refractive index of the intervening medium. The expression in brackets defines the overlap integral **J**, and on evaluation of the constants:

$$R_0 = (9.786\times10^{-5})(\kappa^2\Phi n^{-4}\mathbf{J})^{1/6}\ \text{cm}$$

when λ is expressed in centimeters and $\epsilon_A(\lambda)$ in centimeters squared per millimole. τ is the lifetime of the donor in the absence of acceptor (assuming that the donor decay process is first order), and $\omega(R)dR$ is the probability of finding a particular acceptor at a distance between R and $R + dR$ from the donor. Obviously

$$\omega(R)dR = \omega(r)dr = 2\pi r dr/A_d \quad (3)$$

Using this and the geometrical relationships in Figure 1, $J(t)$ may be reexpressed as

$$J(t) = \frac{2\pi a^2}{A_d}\int_{\theta=0}^{\arctan(r_d/a)} \exp[-(t/\tau)(R_0/a)^6\cos^6\theta]\,\frac{\sin\theta}{\cos^3\theta}\,d\theta \quad (4)$$

Making the substitutions $\alpha = \cos\theta$ and $d\alpha = -\sin\theta\,d\theta$, it is useful to express eq 4 in the form

$$1 - J(t) = \frac{2\pi a^2}{A_d}\int_{\alpha=a/(a^2+r_d^2)^{1/2}}^{1}\{1 - \exp[-(t/\tau)(R_0/a)^6\alpha^6]\}\alpha^{-3}\,d\alpha \quad (5)$$

Since the acceptor concentration is given by

$$c = N/\pi r_d^2 \quad (6)$$

and a concentration c_0 corresponding to one acceptor molecule occupying on average the area of a disk of radius R_0:

$$c_0 = 1/\pi R_0^2 \quad (7)$$

may be defined, eq 5 may be rewritten, including $a/(a^2 + r_d^2)^{1/2} \to 0$ as $r_d \to \infty$, in the form

$$1 - J(t) = (2/N)(c/c_0)(a/R_0)^2\int_{\alpha=0}^{1}\{1 - \exp[-(t/\tau)\times(R_0/a)^6\alpha^6]\}\alpha^{-3}\,d\alpha \quad (8)$$

Expansion of $[J(t)]^N$ in the limit of large N then leads to

$$\bar{p}(t) = \exp\left\{-(t/\tau) - (2/N)(c/c_0)\times(a/R_0)^2\int_{\alpha=0}^{1}(1 - \exp[-(t/\tau)(R_0/a)^6\alpha^6])\alpha^{-3}\,d\alpha\right\} \quad (9)$$

The energy transfer efficiency, E, is given by

$$E = 1 - \int_0^\infty \bar{p}(t)\,dt/\int_0^\infty \rho_0(t)\,dt \quad (10)$$

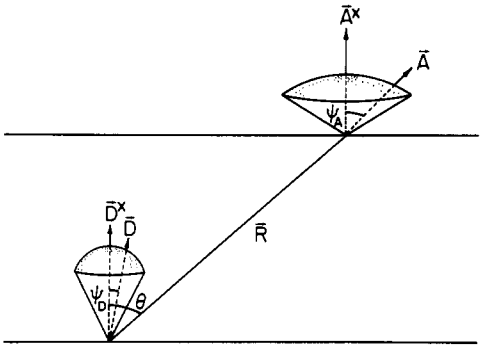

FIGURE 2: Schematic of orientational relationships for donor and acceptor at different levels in a phospholipid bilayer. The axes $\vec{D}^x$ and $\vec{A}^x$ are parallel to each other and normal to the plane of the bilayer. The distributions of donor emission $\vec{D}$ and acceptor absorption $\vec{A}$ transition moment vectors making angles ψ_D and ψ_A with $\vec{D}^x$ and $\vec{A}^x$, respectively, are axially symmetric about them. Here, the distributions are represented as being confined within the volumes of cones, but the specific form of the axially symmetric distribution is unimportant in this context.

where $\rho_0(t) = \exp(-t/\tau)$ is the decay of the donor in the absence of transfer, leading, after substitution of $x = t/\tau$, to

$$E = 1 - \int_{x=0}^{\infty} \exp\left\{-x - (2/N)(c/c_0) \times (a/R_0)^2 \int_{\alpha=0}^{1} (1 - \exp[-(R_0/a)^6 \alpha^6 x])\alpha^{-3}\, d\alpha\right\} dx \quad (11)$$

Although eq 11 could be further developed in terms of incomplete Γ functions, no particular advantage in its integration is thus gained, either in this form or in the more complicated functions resulting from taking the anisotropic orientational dependence of R specifically into account (q.v.). Within the accuracy of numerical integration, it is equivalent to eq 22 of Wolber & Hudson (1979).

Orientational Dependence of FRET Efficiency. The donor emission and acceptor absorption transitions are taken to have orientational distributions which are radially symmetric about axes parallel to the bilayer normal, e.g., as represented pictorially in Figure 2 for the wobbling in cone case (Kinosita et al., 1977), although only the symmetry and not the detail of the distribution is important in the present application. If reorientation within these distributions is rapid in comparison with the transfer rate, a dynamic average value of the orientation factor is appropriate. The general expression (Dale et al., 1979) reduces for the case in hand to

$$\langle\kappa^2(\theta)\rangle = (1 - 3\cos^2\theta)^2\langle d_D^x\rangle\langle d_A^x\rangle + (1/3)(1 - \langle d_D^x\rangle) + (1/3) \times (1 - \langle d_A^x\rangle) + \cos^2\theta[\langle d_D^x\rangle(1 - \langle d_A^x\rangle) + \langle d_A^x\rangle(1 - \langle d_D^x\rangle)] \quad (12)$$

where the so-called axial dopolarization factors, $\langle d_D^x\rangle$ and $\langle d_A^x\rangle$, are given by

$$\langle d_{D,A}^x\rangle = \tfrac{3}{2}\langle\cos^2\psi_{D,A}\rangle - \tfrac{1}{2} \quad (13)$$

The strong dependencies of $\langle\kappa^2(\theta)\rangle$ on θ for a number of combinations of limiting values of $\langle d_D^x\rangle$ and $\langle d_A^x\rangle$ are illustrated in Figure 3. The orientation factor appears explicitly in the Förster separation R_0 and is directly separable from its sixth power:

$$R_0^6 = \langle\kappa^2\rangle R_0'^6 \quad (14)$$

Its effect on the transfer efficiency is limited to the inner

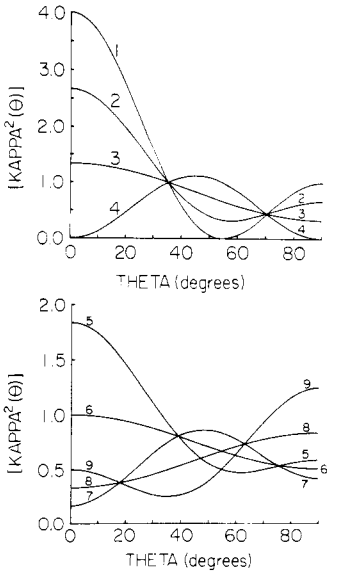

FIGURE 3: Angular dependence of the orientation factor $\langle\kappa^2(\theta)\rangle$ for the donor–acceptor pair in different planes (see eq 12 and Figure 2). Combinations of certain limiting values of the axial depolarization factors $\langle d_D^x\rangle$ and $\langle d_A^x\rangle$ for the donor and acceptor transition moment distributions are presented by way of illustration: (1) 1.0 and 1.0, (2) 1.0 and 0.5, (3) 1.0 and 0, (4) 1.0 and −0.5, (5) 0.5 and 0.5, (6) 0.5 and 0, (7) 0.5 and −0.5, (8) 0 and −0.5, and (9) −0.5 and −0.5. The value of the orientation factor at $\theta = 90°$ is that for the in-plane case.

integral in eq 11 which becomes after appropriate substitutions and some rearrangement

$$E = 1 - \int_{x=0}^{\infty} \exp\left\{-x - (2/N)(c/c_0')(a/R_0')^2 \int_{\alpha=0}^{1} (1 - \exp[-(R_0'/a)^6(A + B\alpha^2 + C\alpha^4)\alpha^6 x])\alpha^{-3}\, d\alpha\right\} dx \quad (15)$$

with c_0' defined on R_0', analogously to c_0 in eq 7, while A, B, and C are functions of $\langle d_D^x\rangle$ and $\langle d_A^x\rangle$:

$$A = \langle d_D^x\rangle\langle d_A^x\rangle + \tfrac{1}{3}(1 - \langle d_D^x\rangle) + \tfrac{1}{3}(1 - \langle d_A^x\rangle)$$
$$B = \langle d_D^x\rangle + \langle d_A^x\rangle - 8\langle d_D^x\rangle\langle d_A^x\rangle \quad (16)$$
$$C = 9\langle d_D^x\rangle\langle d_A^x\rangle$$

The axial depolarization factors may be estimated from the limiting emission anisotropy (r_∞) of the fluorescence of directly excited donor and acceptor in the bilayer systems. Their depolarization, quantitated by the time dependence of the emission anisotropy, $r(t)$, introduced by Jabloński (1960), is characteristically described [e.g., see Kinosita et al. (1977) and Kawato et al. (1977, 1978)] by

$$r(t) = (r_0 - r_\infty)F(t) + r_\infty \quad (17)$$

where $F(t)$ is a complex function that may reasonably well be approximated in some circumstances by a mono- or biexponential decay, and

$$r_\infty/r_0 = \langle d^x\rangle^2 \quad (18)$$

r_0 for excitation of S_1 is taken in eq 18 to have the fundamental value of 0.4 (Dale et al., 1979). The (dynamic) axial depolarization factor is seen to be equivalent to the order parameter S defined in magnetic resonance (Heyn, 1979; Jähnig, 1979).

If the above equations are to be valid to a good approximation, then (i) the effects of curvature of the bilayer vesicles used in this study must be negligible both on the distance and on the orientation dependence of the energy-transfer efficiency, (ii) the effects of relatively slow restricted reorientational relaxation of donor and/or acceptor (nanosecond time scale rather than subnanosecond) on the transfer efficiency must

be negligible, (iii) the effects of a range of possible inter-D–A plane separations corresponding to a distribution of location of the donor across the bilayer, over which the transfer efficiency given by eq 15 should be appropriately averaged, must be considered, and (iv) any effects of having the acceptor distributed, possibly unequally, on both external and internal faces of the bilayer within which the donor is situated must be taken into account.

An examination of these points is deferred to the Discussion.

Experimental Procedures

Fluorescein isothiocyanate (FITC, isomer 1) and DPH were purchased from Sigma Chemical Co., St. Louis, MO, and Koch Light Laboratories Ltd., Colnbrook, England, respectively, and used without further purification. Thin-layer chromatography (TLC) indicated fluorescent dye purities of greater than 99%. Egg lecithin (Lipid Products, Redhill, Surrey) and DPL and cholesterol (Sigma Chemical Co., St. Louis, MO) were used without purification after TLC assessment on silica gel G plates using chloroform/methanol/water (65:25:4 by volume) for the phospholipids and chloroform/methanol/25% (v/v) aqueous ammonia (100:15:1 by volume) for the cholesterol. Phosphatidylethanolamine (PE) from ovine brain was purchased from Sigma Chemical Co., St. Louis, MO, and purified by silicic acid chromatography according to the method of Hanahan et al. (1957). Purity (>95%) was judged from both single-spot TLC analysis ($R_f \simeq 0.8$) and quantitative analysis of the phosphorus to amino nitrogen ratio (Moore & Stein, 1948) [expected 1:1, observed (1.12 ± 0.10):1]. Purified phospholipids were stored at −10 °C in chloroform under nitrogen. The concentration of phospholipids was determined by phosphorus assay (McClare, 1971). All solvents used were of analytical grade with the exception of tetrahydrofuran (THF) which was purified by distillation over sodium metal and stored under nitrogen.

The fluorescent fluorescein-labeled phospholipid F-PE was synthesized by reaction of the α-amino group of PE with FITC (Davenport, 1981). Aliquots of FITC (29.4 mg total weight) were added to 23.8 mg of PE in 4 mL of THF containing 20 μL of triethylamine over a period of 1 h until the FITC had been added to excess (phospholipid to dye molar ratio of 1:2). A similar, independent preparation of fluoresceinthiocarbamyldioleylphosphatidylethanolamine has also been reported (Struck & Pagano, 1980). The reaction was performed in the absence of light, at room temperature under nitrogen and with continuous stirring. The progress of the labeling procedure was followed by TLC on silica gel plates with chloroform/methanol/water (65:25:4 by volume) as the developing solvent. The reaction was judged to have reached completion when no free, underivatized PE was detected, observed by the disappearance of the positive ninhydrin staining spot concurrent with the appearance of a fluorescent spot which also stained positive for phosphorus by using a phosphorus/molybdenum spray reagent (Dittmer & Lester, 1964). The reaction was terminated by applying the mixture to a Sephadex LH-20 (Pharmacia) column (1.8 × 17.2 cm, $V_t \simeq 44$ mL), run under nitrogen and in the absence of light. With THF as the eluting solvent, free unconjugated FITC was well separated from the lipid conjugate, the elution being followed by TLC using ninhydrin and molybdenum spray reagents and by fluorescence. THF was removed by evaporation under reduced pressure and the remaining pale yellow phospholipid residue redissolved in chloroform for further purification from free fatty acids and lyso products by preparative TLC on heat-activated silica gel G plates (20 × 20 cm) using chloroform/methanol/water (65:25:4 by volume) in the dark. The fluorescent conjugate ($R_f \simeq 0.77$) was recovered from the plate by elution with THF. Residual silica gel was removed from the eluate by centrifugation at 5000 rpm in an MSE Minor bench centrifuge for 10 min. The resulting product was judged to be pure (>98%) by TLC using ninhydrin and phosphorus/molybdenum spray reagents and fluorescence as well as by quantitative analysis of its phosphorus to nitrogen ratio (Sloane-Stanley, 1967) [expected 1:2, observed 1:(2.17 ± 0.24)].

Preparation of Phospholipid Vesicles Containing Fluorescent Donor and Acceptor Molecules. Single-bilayer vesicles were prepared by sonication and ultracentrifugation according to Barenholz et al. (1977), using 0.01 M Tris·HCl containing 0.1 M sodium chloride at pH 8.5 as buffer. Sonication was performed under nitrogen and on ice for EL, and at 50 °C (above its phase transition) for DPL, using an MSE sonifier at 12 μm and intermediate power output. Mixed vesicles containing DPL and cholesterol, intimately mixed by colyophilization of the lipid material from chloroform, were also prepared in this way. Single-bilayer vesicles were isolated by centrifugation for 1 h at 108000*g* (30000 rpm) at 15 °C using an MSE 75 high-speed ultracentrifuge. The uppermost fraction of the supernatant was used for the energy-transfer studies.

With the use of a 1.1 mM solution of F-PE in THF and a 1 mM solution of DPH in THF, vesicles were labeled by stepwise addition from a microsyringe into a vortexing suspension (3 mL) of vesicles containing 1 mM total phospholipid to give final donor and acceptor concentrations never greater than 3 μM. The labeled suspensions were incubated at room temperature for approximately 2 h to ensure complete uptake of the fluorescent dyes, as indicated by the lack of any further increase in fluorescence intensity with time. THF was evaporated off by passing a gentle stream of nitrogen over the suspensions. That the F-PE was quantitatively incorporated into the vesicles was demonstrated by correspondence of the scatter and fluorescence peaks observed on monitoring the elution of such suspensions through Sephadex G-25 (Pharmacia) and lack of detectable fluoresence elsewhere in the eluate.

The size distribution of the phospholipid vesicles and possible perturbation after labeling with the fluorescent phospholipid analogue were assessed by electron microscopy (EM) using negative-staining techniques as described elsewhere (Castle & Hubbell, 1976).

For the primary FRET measurements, four aliquots of a sample of each desired phospholipid composition were labeled with (1) DPH only, (2) F-PE only, (3) both DPH and F-PE, and (4) THF solvent alone to give energy-transfer solutions with a constant donor to acceptor molar ratio of 1:1 and a donor or acceptor to phospholipid molar ratio of 1:1000, 1:750, 1:500, 1:428, and 1:350. Samples were quantitatively diluted after incubation to give an absorbance at the wavelength of excitation of either the donor or the acceptor (360 and 500 nm, respectively) of less than 0.02, including vesicle scatter. Duplicates of each vesicle sample, including the blank, were measured in all cases.

Fluorescence Measurements. Steady-state fluorescence excitation and emission spectra were obtained by using a Perkin-Elmer MPF-2A fluorescence spectrophotometer in the ratio mode. An appropriately oriented quartz wedge depolarizer was mounted in the excitation path, and an HNP′B UV-transmitting dichroic film polarizer (Polaroid Corp. Inc.) sandwiched between quartz plates was placed in the observation path between the cuvette and collection lens and or-

ienting at the "magic" angle of ~55° to the symmetry axis which lies along the excitation direction (Spencer & Weber, 1970) in order to obviate polarization bias in the recorded emission intensities. Excitation and emission spectra were corrected for distortion by the wavelength dependence of the illuminating and detection systems, respectively, by making use of a magnesium oxide screen and an 8 g/L rhodamine B in ethylene glycol quantum-counting solution (Yguerabide, 1968), following the methods of Parker & Rees (1960). The correction curve for excitation was checked with a series of dilute fluorescent dye solutions ($A_{\lambda_{max}} < 0.02$) over the wavelength range of interest. The excitation and emission bandwidths were 4 and 3 nm, respectively, for emission spectra and 3 and 4 nm, respectively, for excitation spectra. Spectra were measured at 27.8 ± 0.5 °C for DPL samples (below its phase transition temperature, T_c) and for EL, and at 51.2 ± 0.5 °C for DPL (above its T_c). The peak absorbance of the samples for fluorescence measurements was less than 0.02 to obviate inner filter effects. The quantum yields for donor and acceptor adsorbed to vesicles were determined at both temperatures of interest. For DPH, comparison was made with a nitrogen-purged standard solution of 9,10-diphenylanthracene in cyclohexane [quantum yield ≃ 1 (Ware & Rothman, 1976)] whereas for F-PE a standard solution of fluorescein in 0.1 M NaOH [quantum yield 0.93 ± 0.05 (Weber & Teale, 1957)] was used. The optical densities of the sample and standard were matched at the wavelength of excitation.

Steady-state fluorescence emission anisotropies were measured on the MPF-2A by selecting appropriate polarizations in both the excitation and emission beams using polarizers of the type already described, mounted between the cuvette and the focusing and collecting lenses, respectively. The steady-state emission anisotropy, $\langle r \rangle$, was calculated from

$$\langle r \rangle = \frac{GI_{VV} - I_{VH}}{GI_{VV} + 2I_{VH}} \quad (19)$$

where $G = I_{HH}/I_{HV}$ and represents a correction factor for the inequality of sensitivity of the detection system to horizontally and vertically polarized emission. The first subscript, V or H, refers respectively to the vertical or horizontal orientation of the electric vector of excitation and the second to those for emission.

The location of F-PE in the vesicles was determined by using the quenching of the acceptor probe fluorescence by the heavy iodide anion which does not appreciably penetrate into or through the bilayer (Stubbs et al., 1976). Ten-microliter aliquots of 5 M potassium iodide solution in Tris·HCl buffer were added to vesicle suspensions which were left to incubate for about 15 min before their fluorescence intensities were measured at excitation and emission wavelengths of 490 and 520 nm at bandwidths of 4 and 3 nm, respectively. Background and scatter intensities were measured on a blank sample with no iodide added and subtracted from the readings for all the other samples, allowing for dilution.

Results

Spectroscopic Characteristics of Fluorescently Labeled Phosphatidylcholine Vesicles. During the labeling of vesicles with F-PE, the fluorescence emission anisotropy, which is initially close to zero, reached a maximum value of about 0.1 within about 10 min. By contrast, the fluorescence intensity took about an hour to maximize. This rules out the presence of significant energy transfer between the acceptor fluorophore molecules in the equilibrated state and also indicates the probable absence of significant progressive conformational changes in the liposome as more F-PE (up to 1 per 50 lipid molecules) enters the bilayer.

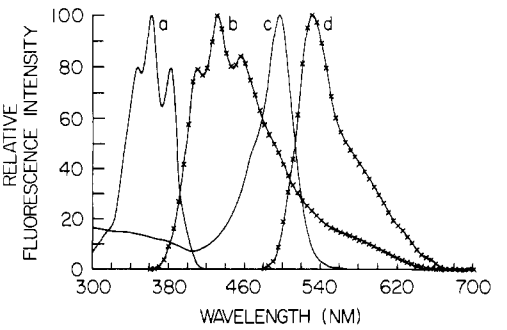

FIGURE 4: Corrected excitation (—) and emission (×) spectra for the donor, DPH (spectra a and b, respectively), and the acceptor, F-PE (spectra c and d, respectively), in DPL vesicles (at a molar labeling ratio of 1:500 probe to phospholipid) at 27.8 ± 0.5 °C.

Table I: Values for the Reference Distance (R_0') for the Donor–Acceptor Pair Oriented in Different Phospholipid Vesicles and at Different Temperatures[a]

phospholipid	temp (°C) (±0.5 °C)	Φ_{DPH}	R_0' (Å) (±1.5 Å)
DPL	27.8	0.50 ± 0.05	46.5
DPL	51.2	0.35 ± 0.04	44.0
DPL/cholesterol (4:1)	27.8	0.50 ± 0.05	46.5
DPL/cholesterol (4:1)	51.2	0.50 ± 0.05	46.5
DPL/cholesterol (2:1)	27.8	0.56 ± 0.06	47.5
DPL/cholesterol (2:1)	51.2	0.56 ± 0.06	47.5
EL	27.8	0.56 ± 0.06	47.5

[a] The values for R_0' are independent of the orientation factor κ^2.

Negative-staining EM of the unlabeled EL and DPL vesicle preparations showed them to consist of single-bilayer vesicles with an average diameter of 250-300 Å. Incorporation of up to 1 F-PE per 50 phosphatidylcholine molecules did not elicit any significant change in vesicle size distribution or bilayer architecture.

The excitation and emission spectra for DPH and F-PE in vesicles are shown in Figure 4. A 13-nm shift to long wavelengths was observed in the emission spectrum of F-PE in vesicles compared to free fluorescein in aqueous alkali and may be attributable to a pH effect or a change in the solvent dielectric constant for the vesicle compared to 0.1 M sodium hydroxide (Martin, 1975). The extinction coefficient at the absorption peak (495 nm) was (6.4 ± 0.5) × 10^4 cm^2 $mmol^{-1}$. The emission spectrum of DPH overlaps well with the absorption spectrum of F-PF, giving an overlap integral J = (8.8 ± 0.7) × 10^{-14} cm^6 $mmol^{-1}$. The donor quantum yields, Φ, measured at a labeling ratio of 1 per 500 lipids, were approximately 30% lower than the reported quantum yield value of 0.8 for DPH in hexane (Shinitzky & Barenholz, 1974), consistent with the shorter average lifetime observed for DPH when incorporated into bilayer vesicles compared with paraffinic solvents (Kawato et al., 1977). They are presented, along with the R_0' values calculated according to eq 2 and 14, using a refractive index of 1.40 as a representative average value between that of the bilayer interior, 1.44 (Badley, 1976), and the aqueous evironment of the acceptor, in Table I. In the absence of donor, the absorption spectrum for the acceptor corresponds closely to its (corrected) excitation spectrum at labeling ratios of less than 1 per 350 phospholipid molecules. At higher acceptor concentrations, the absorbance decreases, and the absorption spectra show broadening and the appearance of a more marked shoulder on the low-wavelength side of the visible absorption maximum, indicative of the formation

of fluorescein dimers. These are nonfluorescent and are not detected in the excitation spectra. As already indicated above, all energy-transfer measurements were performed with acceptor labeling ratios of less than 1 per 350 phospholipids, where no significant fraction of dimer species is detected.

Potassium iodide was observed to quench the fluorescence of the acceptor probe. Stern–Volmer plots of the quenching data are nonlinear for both the DPL and EL vesicles containing adsorbed probe and show a marked leveling off of quenching efficiency with iodide concentration, indicative of inaccessibility of a fraction of the fluorophores to the quencher. Modified Stern–Volmer plots (Lehrer, 1971) for these data are linear. 83 ± 8% and 71 ± 7% of the F-PE molecules in DPL and EL vesicles, respectively, were determined from them to be accessible to quenching by iodide anion. The inaccessible fluorescein sites are presumably on the inner leaflet of the bilayer to which the fluorescently labeled PE has been transferred by "flip-flop". It might have been expected that only a small percentage of such labeled phospholipids would have reached the inside of the bilayer in these experiments, since translocation of phospholipids generally occurs on a time scale of the order of 10^5 s (Finean et al., 1978). The distribution of phospholipids between the outer and inner leaflets of the bilayer may, however, reach equilibrium in a much shorter time, depending upon various physical parameters, such as packing and interaction properties. This appears to be the case for this phospholipid derivative since, at least for the EL vesicles, its distribution corresponds well with that of the bulk phospholipid, about one-third of which is in the inner leaflet (Huang, 1969).

A value of 4.6 ± 0.2 ns for the lifetime of the free fluorescein, of quantum yield 0.93 ± 0.05, was employed to estimate lifetimes of 3.7 ± 0.4 and 3.0 ± 0.4 ns for the DPL and EL systems, respectively, from the measured quantum yields of 0.75 ± 0.07 and 0.61 ± 0.07, respectively, using the Perrin relationship between lifetime and quantum yield (Perrin, 1929):

$$\tau_1/\tau_2 = \phi_1/\phi_2 \qquad (20)$$

The bimolecular rate constants for iodide quenching of F-PE at the accessible sites were identical within experimental error at (1.1 ± 0.2) × 10^9 M^{-1} s^{-1} for F-PE in DPL vesicles and (1.6 ± 0.4) × 10^9 M^{-1} s^{-1} for EL vesicles.

Steady-state fluorescence emission anisotropies of F-PE in the vesicle systems are fairly low (~0.1) and relatively insensitive to temperature in contrast to those of DPH. For instance, in DPL vesicles at a labeling ratio of 1 per 500 lipids, the anisotropy for DPH at 5 °C is about 0.3 and falls to about 0.07 at 60 °C, the majority of the change occurring within a 10 °C span about the gel–liquid-crystalline phase transition temperature of about 39 °C (see Figure 5). The emission anisotropy of F-PE in this system, on the other hand, changes from about 0.12 at 5 °C to about 0.08 at 60 °C and exhibits only a slight inflection in the region of the phase transition temperature.

The anisotropy of DPH was also measured in both EL and DPL systems with and without cholesterol, above and below the phase transition temperature in the case of DPL. The results for a labeling ratio of 1 to 500 are presented in Figure 5. It is evident that, while the orientational constraints on the acceptor fluorophore were essentially the same for all the systems, as estimated from its steady-state emission anisotropy, a considerable range of constraints was encountered for the donor.

Steady-State Fluorescence Measurements of Excitation Energy Transfer in Phospholipid Vesicles. Examples of

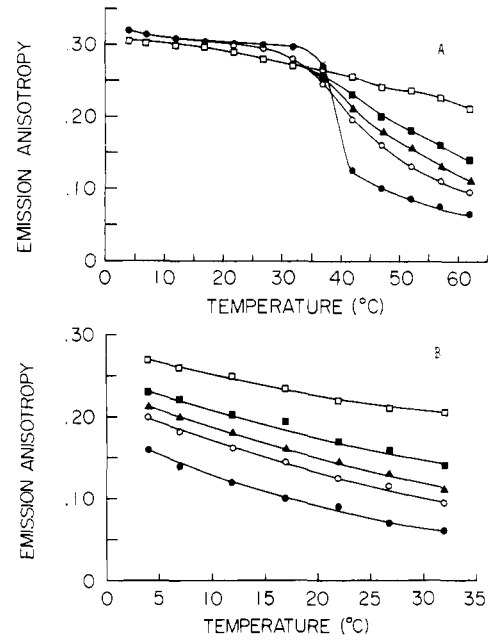

FIGURE 5: Steady-state emission anisotropy as a function of temperature for DPH incorporated into (A) DPL vesicles and (B) EL vesicles at varying cholesterol concentrations: (●) phospholipid alone; (○) phospholipid/cholesterol (molar ratio 4:1); (▲) phospholipid/cholesterol (3:1); (■) phospholipid/cholesterol (2:1), and (□) phospholipid/cholesterol (1:1). A molar labeling ratio for DPH to total lipid of 1:500 was employed.

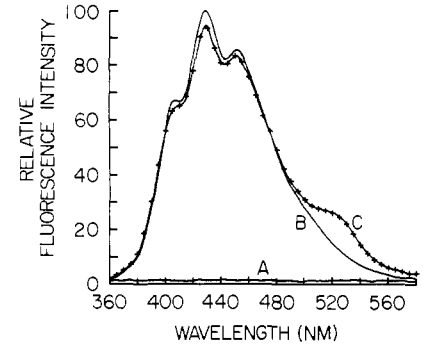

FIGURE 6: Example of experimental emission spectral energy-transfer data for F-PE- and DPH-labeled DPL vesicles (at a molar labeling ratio of 1:500 probe to phospholipid). The designations A, B, and C refer to blank, donor alone, and donor and acceptor together, respectively. Excitation was at 360 nm, with excitation and emission bandwidths of 4 and 3 nm, respectively.

emission spectra for the donor-labeled vesicles in the presence and absence of acceptor are shown in Figure 6. A series of experiments with increasing donor to phospholipid ratios and a constant donor to acceptor ratio of unity were carried out. As the concentration of fluorophore increases, the fluorescence intensity of DPH at 430 nm decreases relative to its value in the absence of acceptor, while the intensity of F-PE fluorescence at 520 nm increases when predominantly DPH is excited in its main near-UV absorption band at 360 nm. Both of these effects are attributable to excitation energy transfer from donor DPH to acceptor F-PE.

The dependence of the energy-transfer efficiency (E) on the acceptor concentration was determined via the excitation spectrum of the acceptor. Measured spectra (e.g., Figure 7) were fully corrected for vesicle scatter and fluorescence, for donor emission at the acceptor observation wavelength, and for instrumental excitation efficiency. These corrected excitation spectra were compared with the sum of the absorption spectra pertaining to donor and acceptor in the transfer sample

Table II: Comparison of Electronic Excitation Energy-Transfer Efficiencies Determined by the Decrease in Donor Emission Fluorescence Intensity (E_{em}) and by Sensitization of Acceptor Emission (E_{ex}) Using Excitation Spectra

vesicle type	molar labeling ratio[a]	temp (°C) 27.8 ± 0.5 E_{ex}	27.8 ± 0.5 E_{em}	51.2 + 0.5 E_{ex}	51.2 + 0.5 E_{em}
EL	1:1000	0.05 ± 0.01	0.09 ± 0.01		
	1:750	0.07 ± 0.02	0.15 ± 0.02		
	1:500	0.11 ± 0.03	0.14 ± 0.01		
	1:428	0.11 ± 0.05	0.15 ± 0.02		
	1:350	0.12 ± 0.02	0.20 ± 0.06		
DPL	1:1000	0.08 ± 0.01	0.09 ± 0.03	0.05 ± 0.02	0.05 ± 0.02
	1:750	0.10 ± 0.01	0.12 ± 0.05	0.075 ± 0.015	0.06 ± 0.02
	1:500	0.14 ± 0.02	0.14 ± 0.05	0.11 ± 0.02	0.075 ± 0.015
	1:428	0.17 ± 0.02	0.12 ± 0.04	0.12 ± 0.02	0.09 ± 0.03
	1:350	0.21 ± 0.02	0.14 ± 0.02	0.16 ± 0.02	0.125 ± 0.035
DPL/cholesterol (4:1)	1:1000	0.065 ± 0.01	0.07 ± 0.01	0.05	0.07
	1:750	0.09 ± 0.01	0.095 ± 0.005	0.09	0.11
	1:500	0.135 ± 0.01	0.14 ± 0.01	0.13	0.13
	1:428	0.195 ± 0.005	0.22 ± 0.06	0.19	0.17
DPL/cholesterol (2:1)	1:1000	0.04 ± 0.005	0.075 ± 0.005	0.06	0.07
	1:750	0.07 ± 0.005	0.09 ± 0.04	0.08	0.11
	1:500	0.235 ± 0.005	0.36 ± 0.04	0.18	0.29
	1:428	0.295 ± 0.005	0.45 ± 0.05	0.29	0.42

[a] The molar labeling ratio refers to the donor–acceptor to phospholipid ratio, the donor to acceptor ratio being 1:1 in all cases.

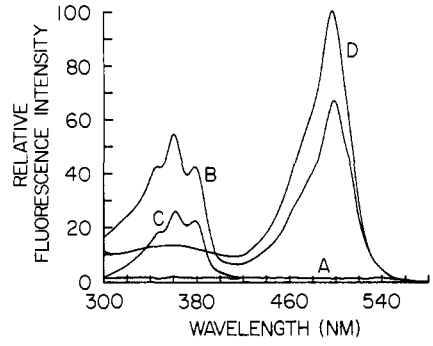

FIGURE 7: Example of experimental excitation spectral energy-transfer data for F-PE- and DPH-labeled DPL vesicles (at a molar labeling ratio of 1:500 of each probe to phospholipid). The designations A, B, C, and D refer to blank, donor and acceptor together, donor alone, and acceptor alone, respectively. Emission was observed at 550 nm with excitation and emission bandwidths of 4 and 6 nm, respectively.

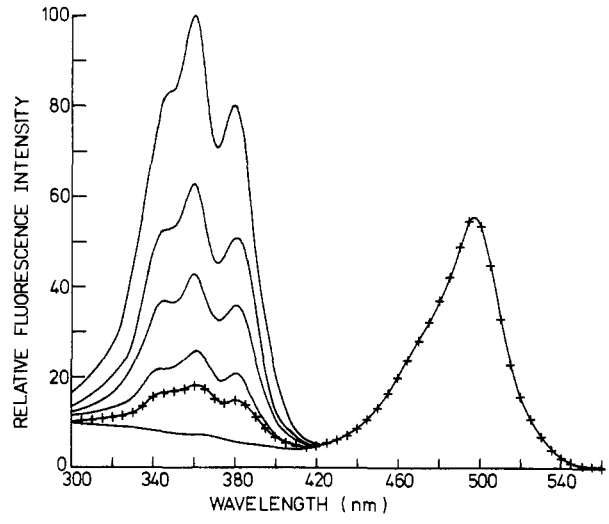

FIGURE 8: Theoretical excitation spectra for various energy-transfer efficiencies (0, 0.2, 0.4, 0.6, and 1 in order of increasing signal in the donor excitation region) from the donor DPH to the acceptor F-PE. (+) shows the fully corrected experimental excitation spectrum for donor- and acceptor-labeled DPL vesicles (molar probe to phospholipid ratio of 1:500 and F-PE to DPH ratio of 1:1) with an energy-transfer efficiency of 0.12 at 27.8 ± 0.5 °C.

(equivalent to the excitation spectrum that would be observed for 100% efficient transfer to the acceptor), with that of the acceptor monomer alone (equivalent to the excitation spectrum for 0% transfer), and with those including intermediate fractions (f) of donor absorption between these levels (corresponding to the excitation spectra which would be observed for transfer efficiencies $E = f$), an example being shown in Figure 8. The excitation spectrum in the absence of donor is virtually identical with the absorption spectrum of F-PE. As the concentration of donor was increased, excitation peaks around 360 nm arising as a result of energy transfer were observed. The transfer efficiencies (E_{ex}) determined in this way for vesicles of DPL, with and without cholesterol at 20 and 33 mol %, above and below the phase transition, and for egg lecithin vesicles are summarized in Table II.

Since all the fluorescence at 430 nm arises from DPH, the efficiency of energy transfer can also readily be calculated from the quenching of donor fluorescence:

$$E_{em} = 1 - F/F_0 \qquad (21)$$

where F is the fluorescence intensity of DPH at 430 nm measured in the presence of F-PE compared with F_0, the intensity in the absence of F-PE. While these results agreed with the excitation spectral data to within 2 standard deviations in all cases, they were in general very much less reproducible and consistent than the former (Table II). This appears to arise from their critical dependence on the ratio of intensities in two separate samples; for the excitation measurements, it is the ratio of intensities within a single sample that predominantly determines the result.

Transfer efficiencies were also measured as a function of donor concentration over the range of 1–9 per 1500 phospholipid molecules at a constant acceptor concentration of 3 per 1500 phospholipids for the pure DPL systems and were found to be independent of donor concentration. This implies the absence of significant interdonor ("self-") transfer (Fung & Stryer, 1978) and, at least in these cases, justifies the assumption made implicitly in the derivation of eq 11 for the FRET efficiency.

The transfer efficiencies obtained in each of the cholesterol-free phospholipid systems labeled at a ratio of 1 to 500

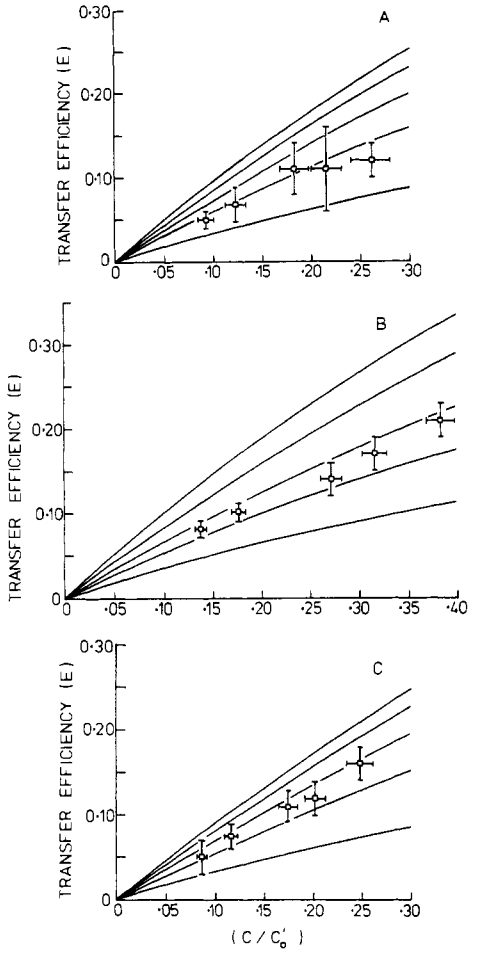

FIGURE 9: Excitation energy-transfer efficiency (E) as a function of acceptor concentration for DPH and F-PE at a 1:1 molar ratio in (A) EL vesicles at 27.8 ± 0.5 °C, (B) DPL vesicles at 27.8 ± 0.5 °C, and (C) DPL vesicles at 51.2 ± 0.5 °C. The donor and acceptor axial depolarization factors were taken to be (A) 0.2 and 0.5, respectively, (B) 0.9 and 0.5, respectively, and (C) 0.3 and 0.5, respectively. Theoretical solutions are shown for donor–acceptor plane separations (a/R_0'), reading from top to bottom in each case, of 0 (in plane), 0.3, 0.5, 0.7, and 1. The same set of molar probe to phospholipid ratios was used in each case. The concentration scales for the data points differ by virtue of the different areas per phospholipid head group used: 77 ± 6 Å^2 for EL, 50 ± 2 Å^2 for DPL below T_c, and 70 ± 4 Å^2 for DPL above T_c.

are presented as functions of the reduced concentration (c/c_0') in Figure 9. The surface concentrations of acceptor were estimated from the F-PE to phospholipid ratio in these preparations by using data on the surface area per phospholipid head group culled from the literature. As reflected in the horizontal error bars in Figure 9 (reflecting maximum and minimum estimates), there is considerable uncertainty in these values. They were taken to correspond to overall surface areas per phospholipid head group of 77 ± 6 Å^2 for EL [Huang, 1969; see also Parsegian et al. (1979) and Cornell & Separovic, (1983)], 50 ± 2 Å^2 for DPL at 28 °C (Janiak et al., 1979; Rand et al., 1980), and 70 ± 4 Å^2 for DPL at 51 °C [see Cornell & Separovic (1983)].

In each of the plots are also presented the theoretical FRET efficiency curves for a range of a/R_0', the ratio of the interplane separation to the (reduced) Förster separation, between 0 and 1. They change from plot to plot because of the difference in $\langle\kappa^2(\theta)\rangle$ arising from the variation in the extent to which the donor can reorient in the different systems, expressed by the axial depolarization factor $\langle d_D^x\rangle$. Values of the latter both used here and used for the DPL cholesterol systems (see

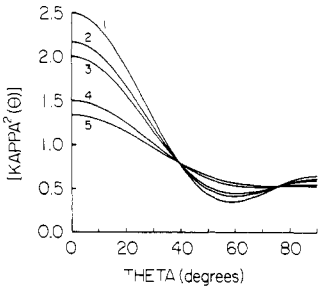

FIGURE 10: Orientation factor $\langle\kappa^2(\theta)\rangle$ for a two-dimensional out of plane donor–acceptor pair as a function of the angular separation θ. Combinations of the axial depolarization factors for the donor $\langle d_D^x\rangle$ with a constant $\langle d_A^x\rangle$ of 0.5 for the acceptor corresponding to the cases of interest here are presented: (1) 0.9, (2) 0.7, (3) 0.6, (4) 0.3, and (5) 0.2. It is noted that, for the most important range of θ, near 0, $\langle\kappa^2(\theta)\rangle$ takes on values of between about 2- and nearly 4-fold the random dynamic average of $^2/_3$ in the various systems investigated here.

Table III: Summary of Apparent Donor–Acceptor Plane Separations (a) as a Function of Vesicle Type and Temperature[a]

vesicle type	temp (±0.5 °C) 27.8 a/R_0'	27.8 a (Å)	51.2 a/R_0'	51.2 a (Å)
EL	0.72 ± 0.04	34 ± 2		
DPL	0.60 ± 0.05	28 ± 2.5	0.55 ± 0.05	24 ± 2.5

[a] Quoted to nearest 0.5 Å.

Figure 11) were estimated by using eq 18 from time-resolved depolarization data reported in the literature (Kawato et al., 1977, 1978). The axial depolarization factor (d_A^x) corresponding to restricted motion of the fluorescein moiety of F-PE in the various vesicles was essentially the same, having a value close to 0.5, in all cases. These values were estimated on the assumption that essentially all the depolarization observed was due to rapid reorientational relaxation of the dye moiety opposed only by the low viscosity of the aqueous medium, over a range restricted by the vesicle surface. This assumption is strongly supported by the lack of significant temperature dependence of its depolarization. The effects of restricted reorientation of D and A on $\langle\kappa^2(\theta)\rangle$ for the cases obtained here are presented in Figure 10. The apparent values of a/R_0' for interpolated FRET curves best approximating the pure phospholipid data are summarized in Table III.

In contrast to these results, the data for the cholesterol-loaded DPL vesicles (Figure 11) appear anomalous. In the absence of data on the average surface area occupied by the phospholipid head groups in these systems, the measured transfer efficiencies are presented, both above and below the phase transition temperature, on reduced concentration scales corresponding to 94 ± 7 and 70 ± 4 Å^2 for the 20 and 33 mol % cholesterol systems, respectively, taken from data on EL/cholesterol vesicles (Newman & Huang, 1975) for arbitrary reference. It can readily be seen that, whatever the (reasonable) concentration scales employed, the transfer efficiencies at high acceptor concentrations become impossibly high relative to those at low acceptor concentrations.

Discussion

As an energy-transfer pair, the donor DPH and acceptor F-PE satisfy all the necessary requirements for efficient FRET, the donor emission spectrum having appreciable overlap with the acceptor absorption spectrum, the donor quantum yield being also reasonably high. The values of the reduced Förster separation (R_0') determined are all on the order of 45 Å, which

Table IV: Phospholipid Bilayer Characteristics Derived from X-ray Diffraction and Scattering Data in the Literature

		full width, d (Å)	peak to peak width, d_1 (Å)	$d-d_1$ (Å)[a]	ref
EL	oriented multibilayers	46	38	8	Levine & Wilkins (1971)
	sonicated dispersions	44	36	(8)	Wilkins et al. (1971)
	multibilayer dispersions	43	35	(8)	Parsegian et al. (1979)
DPL ($T < T_c$)	oriented multibilayers	58	46	12	Levine et al. (1968)
	multibilayer dispersions	50	42	8	Inoko & Mitsui (1978)
	sonicated dispersions[a]	55	44.5	10.5	Herbette et al. (1984)
	multibilayer dispersions	58	48	(10)	Janiak et al. (1976)
	multibilayer dispersions	52	42	(10)	Rand et al. (1980)
DPL ($T > T_c$)	multibilayer dispersions	47	39	8	Inoko & Mitsui (1978)
	multibilayer dispersions	43	35	(8)	Janiak et al. (1976)
	multibilayer dispersions	42	34	(8)	Lis et al. (1982)
	sonicated dispersions	45	37	(8)	Lewis & Engelman (1983)

[a] Figures for $d-d_1$ in parentheses are assumed values corresponding to those measured where available, an average in the case of DPL at $T < T_c$.

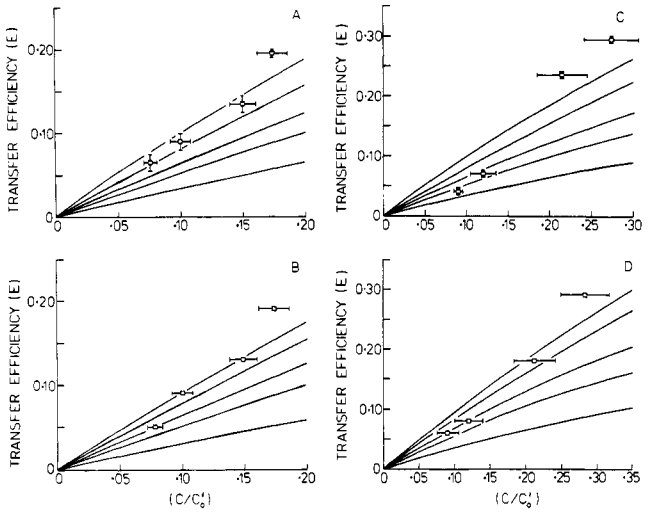

FIGURE 11: Excitation energy-transfer efficiency (E) as a function of acceptor concentration for DPH and F-PE at a 1:1 molar ratio in (A) DPL/cholesterol (20 mol %) vesicles at 27.8 ± 0.5 °C, (B) DPL/cholesterol (20 mol %) vesicles at 51.2 ± 0.5 °C, (C) DPL/cholesterol (33 mol %) vesicles at 27.8 ± 0.5 °C, and (D) DPL/cholesterol (33 mol %) vesicles at 51.2 ± 0.5 °C. The donor and acceptor axial depolarization factors were taken to be (A) 0.9 and 0.5, respectively, (B) 0.6 and 0.5, respectively, (C) 0.9 and 0.5, respectively, and (D) 0.7 and 0.5, respectively. Theoretical solutions for donor–acceptor plane separations (a/R_0') of 0 (in plane), 0.3, 0.5, 0.7, and 1, reading top to bottom, are also shown in each case. The concentration scales for the data correspond arbitrarily (see text) to overall areas per phospholipid head group of 94 ± 7 and 70 ± 4 Å^2 for the 20 and 33 mol % cholesterol systems, respectively.

is comparable with most of the current estimates of EL and DPL vesicle bilayer thickness, defined here as the distance across the bilayer encompassing the phosphate groups on both sides, of ~40–60 Å (Levine et al., 1968; Levine & Wilkins, 1971; Wilkins et al., 1971; Janiak et al., 1976; Inoko & Mitsui, 1978; Rand et al., 1980; Lis et al., 1982; Lewis & Engelman, 1983; Herbette et al., 1984). This may be expected, in general, to afford a high degree of sensitivity to the determination of the donor–acceptor interplane separation which must be of the order of half this value [compare Wolber & Hudson (1979)].

The values of apparent donor–acceptor plane separations summarized in Table III should be compared with estimates of half the bilayer widths (inclusive of phosphate head group) plus the projection of the fluoresceinthiocarbamylethanolamine side chain from the surface. From the chemical structure, the maximum projection of the origin of the dipole moment responsible for the energy-transfer-accepting properties from the surface is about 12 Å, the minimum (taking into account the double negative charge on the fluorescein moiety) about 6 Å, a reasonable estimation of the mean separation then being 10 ± 2 Å, again taking into account the negative charge. Bilayer widths in the literature are normally quoted as d_1, the peak to peak electron density separation across the bilayer derived from X-ray diffraction or scattering experiments and supposed to represent the phosphate to phosphate separation. A reasonable estimate of the bilayer width inclusive of phosphate is then obtained by adding twice the external half-width at half-maximum to this value in those cases where figures of electron density are presented. The results of a survey of the literature for these widths are presented in Table IV. The appropriate comparisons with the apparent donor–acceptor plane separations given in Table III are thus 32 ± 3 Å for EL, 37.5 ± 4 Å for DPL below the phase transition temperature, and 32 ± 3 Å for DPL above the phase transition temperature, quoted to the nearest 0.5 Å.

It appears from these comparisons that the physical state of the phospholipid in pure phospholipid vesicles is important in determining the distribution of the donor molecule, DPH, across the bilayer. The estimates obtained for the apparent separation of donor and acceptor planes suggest that, for EL vesicles, the DPH is predominantly located at and in the close vicinity of the center of the bilayer. For DPL both above and below its phase transition temperature, on the other hand, a fairly broad spread about the center is indicated. This difference presumably reflects the heterogeneity of both length and unsaturation of the acyl chains of EL compared with their homogeneity and saturation in the pure synthetic DPL.

Quantitatively, the apparent separations thus calculated represent an average interplane separation corresponding to rapid translational equilibration of the donor DPH over its distribution across the bilayer, no account being taken of the further orientational averaging that this would engender. Within this assumption, further refinement of the transbilayer distribution in terms of the width of, e.g., truncated Gaussian or Lorentzian profiles (rather narrow for EL, rather broad for DPL) is obviously possible. Alternatively, and more reasonably, matching of the data to averages of efficiency curves for ranges of a/R_0' values calculated directly or interpolated from those presented and weighted according to the distribution assumed could be carried out. These results would correspond to slow translational equilibration of the donor over its distribution across the bilayer, would automatically also include the appropriate orientational averaging, and must again lead to a narrow distribution for EL and a broad distribution for DPL. These procedures would not add anything significant to the above analysis (see also further discussion on the dynamic vs. static regimes of equilibration across the bilayer, and see the Appendix), the qualitative interpretation of which is

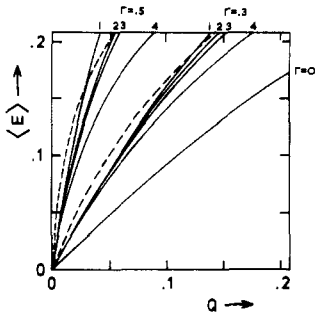

FIGURE 12: Comparison of energy-transfer efficiencies for a linear model analogue of the membrane donor–acceptor system as a function of acceptor potential for dynamic and static positional averaging of the donor with acceptor potential distributed (a) equally on either side of the donor or (b) on one side only. The efficiencies are identical in these two cases when the donor position is dynamically averaged. For a given relative spread ($\pm\Gamma$, $0 \leq \Gamma \leq 1$) of the donor positions about the origin, transfer is most efficient in the dynamic averaging regime and least efficient for the one-sided acceptor location in the static averaging limit for the donor. (—) Sets of the four curves: (1) dynamic donor distribution; (2, 3, and 4) static donor distribution with even, 3:1, and one-sided acceptor distributions, respectively, for $\Gamma = 0$, 0.3, and 0.5. (---) One-sided, static limit curves for $\Gamma = 0.37$ and 0.60 which approximately match the dynamic limit curves for $\Gamma = 0.3$ and 0.5, respectively.

quite clearcut, and they have not been attempted. To be really useful, such analyses would require either steady-state energy-transfer measurements using, e.g., different acceptor molecules giving a fairly wide range of R_0' or detailed analysis of the time course of donor and/or acceptor emission [cf. end to end distance distributions of polymers labeled with suitable donor and acceptor moieties as proposed by Cantor & Pechukas (1971) and by Steinberg and co-workers (Grinvald et al., 1972; Haas et al., 1975, 1978), respectively, proper account being taken of the correlation between interplane separation and the orientation factor].

On the other hand, there is no reason to suppose that translational equilibration of DPH over its distribution across the bilayer *is* rapid, particularly for DPL below T_c. The distribution calculated in full for such a statically averaged system will, in general, be different from that for the equivalent but dynamically averaged distribution that gives the same transfer efficiency. Furthermore, if there is an uneven distribution of acceptor between the two sides of the bilayer (considered for the moment as planar), yet another donor distribution would correspond, in the static limit, to a given transfer efficiency, even though the donor distribution is symmetric about the median bilayer plane. These considerations will obviously not affect the qualitative interpretation of the data discussed above. That they will have little effect also on the quantitative interpretation is illustrated in the Appendix by making use of a simple linear model example in which these effects must be much more extreme than for the systems studied here, since the transfer rates there are directly dependent on the inverse sixth power of the separation, whereas in the bilayer case they average out to something on the order of the inverse square of the average separation.

The presence of cholesterol in the bilayer architecture, at least at the levels of 20 and 33 mol %, is seen to have a striking effect on the observed energy-transfer efficiency at reduced concentrations (c/c_0') greater than about 0.15. The efficiency increases dramatically compared with that predicted on the basis of its values at $c/c_0' < 0.15$. These effects may be rationalized by assuming phase separation of the bilayer components into cholesterol-rich and cholesterol-poor regions either laterally (Shimshick & McConnell, 1973) or transversely (Huang et al., 1974; de Kruijff, 1976) and preferential partitioning of the DPH into one of these phases, giving rise, at high enough labeling ratios, to concentrations of DPH for which appreciable inter-DPH ("self-") transfer can occur, thus leading to an enhanced donor–acceptor transfer efficiency. This hypothesis is at variance with the conclusion drawn from studies on lateral energy transfer between DPH and fluorescent sterol analogues in dimyristoyllecithin and EL vesicles that no segregation of sterols occurs in such systems in the liquid-crystalline state (Wharton et al., 1980). An explanation of the discrepancy may lie in lack of consideration of orientational effects in that study.

The results presented here, along with the relevant theoretical treatment and experimental protocols, indicate how, under appropriate conditions, spatial relationships between membrane components located at different levels across the bilayer may be assessed by the Förster resonance energy-transfer method, specifically taking into account the effects of relative orientations of donor and acceptor. The theoretical expressions used to quantitate the FRET data presented here apply strictly to the case of donors and acceptors restricted to parallel planes separated by a fixed distance in the limit that lateral diffusion is negligibly slow and reorientational diffusion fast in comparison with transfer rates. For the relatively low energy-transfer efficiencies observed in this study, and from the reorientational correlation times of a few nanoseconds reported in the literature for similar vesicle preparations (Kawato et al., 1977, 1978) and an upper bound to the lateral diffusion coefficient of $\sim 10^6$ cm^2/s (Rigaud et al., 1972), the above limiting conditions would appear to be met satisfactorily. By analogy with the effects of curvature on FRET efficiency between donors and acceptors located on the same surface reported previously (Eisinger et al., 1981), considering the orientational restraints obtaining in the present systems, it would appear that the curvature of the vesicles, of diameter about 5 or 6 times the R_0' value, will also have little influence on the transfer efficiency compared with that pertaining to the equivalent planar systems.

The transverse location of the popular probe of membrane structure and fluidity, DPH, determined and reported here for single-bilayer vesicles of EL, and of DPL above and below the phase transition temperature, appears to depend critically on the different physical states of the bilayer interior in these systems. The inferred distribution about the center of the bilayer appears to be quite narrow for EL which is characterized by a physically and chemically heterogeneous internal environment. It is significantly broader for DPL, in which the internal environment is rather homogeneous, both above and below its phase transition. The transverse distribution of the probe appears to be governed by a strong tendency to partition preferentially into highly disordered regions of the bilayer. Where there is minimal disorder, no preference is observed, and the distribution becomes much broader. These considerations are of particular relevance to the interpretation of both steady-state and time-resolved emission anisotropy data for lipid bilayer systems.

ACKNOWLEDGMENTS

We thank T. Marszalek for advice and assistance with modifications to the fluorescence spectrometer used in these measurements. We acknowledge L. Brand for helpful discussions, Nancy Beechem for aid with graphic arts, and Dorothy Regula for her patience in preparing the manuscript. Finally, we particularly record our thanks to Larry A. Sklar for advice on estimates of bilayer width critical to the interpretation of these data.

Appendix

For FRET from donor moieties having some distribution of depth within a phospholipid vesicle bilayer to acceptors situated on the surfaces of the bilayer, both the distribution of the acceptor between the external and internal surfaces and the positional averaging regime, dynamic or static, obtaining for the donor over its distribution across the bilayer, may affect the observable transfer efficiency. Other effects, such as averaging of the orientation factor correlated with depth in the bilayer, reorientational averaging regime, and curvature of the vesicle, may also influence the transfer efficiency and are considered elsewhere in the text. To illustrate the likely extent of the first two factors indicated above, a simple linear analogue is examined in which these effects can be expected to exert a greater influence on the efficiency than in the vesicle system because the distance dependence of the transfer rates is very much sharper in the linear model than for the membrane.

In the model, it is supposed that there exists an ensemble of donor–acceptor systems in each of which there are two locations that can be occupied by acceptors, at distances $\pm R_m$ from an origin about which a donor may occupy any position r in $\pm R$ ($0 \le R \le R_m$) with equal probability. The four cases to be considered are the following: (i) acceptor localized at R_m (or at $-R_m$), donor distribution dynamic; (ii) acceptor equally distributed at R_m and $-R_m$, donor distribution static; (iii) donor as in (i), acceptor as in (ii); (iv) acceptor as in (i), donor as in (ii). In (i) and (iii), all members of the respective ensembles are identical. In (iv), each member of the ensemble is different, while in (ii), pairs of members are equivalent by symmetry.

For a donor at r ($-R \le r \le R$) transferring to an acceptor localized at R_m, the transfer rate is given by

$$k_L = (1/\tau)[R_0/(R_m - r)]^6 \quad \text{(A1)}$$

The sixth power ratio in this equation is analogous to the concentration ratio c/c_0 obtaining in the membrane case and may formally be treated as such and regarded as a normalizing condition. Without loss of generality, then, the rate of transfer to acceptor "potential" equally distributed at R_m and $-R_m$ is given by

$$k_D = (1/\tau)\{\tfrac{1}{2}[R_0/(R_m - r)]^6 + \tfrac{1}{2}[R_0/(R_m + r)]^6\} \quad \text{(A2)}$$

In the dynamic cases, the transfer efficiency depends on the average of the rate k over the donor distribution:

$$\langle E\rangle_d = \langle k\rangle/(1/\tau + \langle k\rangle) \quad \text{(A3)}$$

while in the static cases, it is the efficiency itself which is averaged over the distribution

$$\langle E\rangle_s = \langle k/(1/\tau + k)\rangle \quad \text{(A4)}$$

Writing $Q = (R_0/R_m)^6$ and $\gamma = r/R_m$ and integrating over γ in the range $\pm\Gamma$ ($\Gamma = R/R_m$):

$$\langle k_L\rangle = (1/\tau)\int_{-\Gamma}^{\Gamma} Q(1-\gamma)^{-6}\,d\gamma \Big/ \int_{-\Gamma}^{\Gamma} d\gamma = (Q/10\Gamma)[(1-\Gamma)^{-5} - (1+\Gamma)^{-5}] = \langle k_D\rangle \quad \text{(A5)}$$

from which the transfer efficiencies for the equivalent cases i and iii may be calculated as a function of Q and Γ from eq A3. Similarly, for localized acceptor and a static donor distribution, case iv, combining eq A1 and A4 leads to

$$\langle E\rangle_{sL} = (1/2\Gamma)\int_{-\Gamma}^{\Gamma}\{Q(1-\gamma)^{-6}/[1 + Q(1-\gamma)^{-6}]\}\,d\gamma \quad \text{(A6)}$$

and for the distributed acceptor, case ii:

$$\langle E\rangle_{sD} = (1/\Gamma)\int_0^{\Gamma}\{(Q/2)[(1-\gamma)^{-6} + (1+\gamma)^{-6}]/(1 + (Q/2)[(1-\gamma)^{-6} + (1+\gamma)^{-6}])\}\,d\gamma \quad \text{(A7)}$$

The integrals in eq A6 and A7 were evaluated numerically by using intervals $d\gamma = 0.01\Gamma$, and representative results for transfer efficiences up to about 0.2, corresponding to the highest efficiency measured in the experiments reported here, are presented in Figure 12. These are also compared in the figure with those for the intermediate case of a 3:1 distribution of acceptor between the two sites, corresponding roughly with the distribution of acceptor concentration on the inside and outside of the vesicle bilayer in the experiments reported here for DPL, where the acceptor is partitioned between the outer and inner surfaces at a ratio of about 5:1, whereas the bulk phospholipid is distributed at a ratio of about 2:1 (Huang, 1969).

Remembering that the effects observed in this model are expected to be considerably more severe than those in the real case of interest and that the typical error bars on data points cover ±0.02 in efficiency and ±10% of scale in concentration, it is evident that neither the averaging effects nor the averaging effects due to somewhat unequal acceptor distribution between the inside and outside of the bilayer would be expected to be detectable in the data presented. Certainly, the qualitative conclusions drawn will be unaffected, and even a more extensive quantitative analysis would be expected to change the derived distribution widths by considerably less than the 10% or so indicated here, even for donor distributions with full widths at half-maximum somewhat in excess of half the minimum separation between acceptors across the bilayer.

Registry No. DPH, 1720-32-7; DPL, 2797-68-4; cholesterol, 57-88-5.

References

Andrich, M. P., & Vanderkooi, J. M. (1976) *Biochemistry 15*, 1257–1261.

Badley, R. A. (1976) in *Modern Fluorescence Spectroscopy* (Wehry, E. L., Ed.) Vol. 2, Chapter 3, pp 91–168, Plenum Press, New York.

Barenholz, Y., Gibbes, D., Litman, B. J., Goll, J., Thompson, T. E., & Carlson, F. D. (1977) *Biochemistry 16*, 2806–2810.

Barrett-Bee, K., Radda, G. K., & Thomas, N. A. (1972) *Proc. FEBS Meet., 8th*, 231–252.

Cantor, C. R., & Pechukas, P. (1971) *Proc. Natl. Acad. Sci. U.S.A. 68*, 2099–2101.

Castle, J. D., & Hubbell, W. L. (1976) *Biochemistry 15*, 4818–4831.

Cornell, B. A., & Separovic, F. (1983) *Biochim. Biophys. Acta 733*, 189–193.

Dale, R. E., Eisinger, J., & Blumberg, W. E. (1979) *Biophys. J. 26*, 161–194.

Dale, R. E., Novros, J., Roth, S., Edidin, M., & Brand, L. (1981) in *Fluorescent Probes* (Beddard, G. S., & West, M. A., Eds.) pp 159–181, Academic Press, New York.

Davenport, L. (1981) Ph.D. Thesis, University of Salford, Salford, U.K.

de Kruijff, B., Cullis, P. R., & Radda, G. K. (1976) *Biochim. Biophys. Acta 436*, 729–740.

Dewey, T. G., & Hammes, G. (1980) *Biophys. J. 32*, 1023–1036.

Dittmer, J. C., & Lester, R. L. (1964) *J. Lipid Res. 5*, 126–127.

Eisinger, J., & Flores, J. (1983) *Biophys. J. 41*, 367–379.

Eisinger, J., Blumberg, W. E., & Dale, R. E. (1981) *Ann. N.Y. Acad. Sci. 366*, 155–175.

Fairclough, R. H., & Cantor, C. R. (1978) *Methods Enzymol. 48*, 378–425.
Finean, J. B., Coleman, R., & Michell, R. H. (1981) *Membranes and Their Cellular Functions*, 2nd ed., Blackwell Scientific Publications, Oxford, U.K.
Fleming, P. J., Koppel, D. E., Lau, A. L. Y., & Strittmatter, P. (1979) *Biochemistry 18*, 5458–5464.
Förster, Th. (1949) *Z. Naturforsch., A: Astrophys., Phys. Phys. Chem. 4A*, 321–327.
Fung, B. K.-K., & Stryer, L. (1978) *Biochemistry 17*, 5241–5248.
Gent, M. P. N., & Pretegard, J. H. (1974) *Biochemistry 13*, 4027–4032.
Grinvald, A., Haas, E., & Steinberg, I. Z. (1972) *Proc. Natl. Acad. Sci. U.S.A. 69*, 2273–2277.
Haas, E., Wilchek, M., Katchalski-Katzir, E., & Steinberg, I. Z. (1975) *Proc. Natl. Acad. Sci. U.S.A. 72*, 1807–1811.
Haas, E., Katchalski-Katzir, E., & Steinberg, I. Z. (1978) *Biopolymers 17*, 11–31.
Haigh, E. A., Thulborn, K. R., & Sawyer, W. H. (1979) *Biochemistry 18*, 3525–3532.
Hanahan, D. J., Dittmer, J. C., & Warashina, E. (1957) *J. Biol. Chem. 228*, 685–700.
Hartmann, W., Galla, H.-J., & Sackmann, E. (1978) *Biochim. Biophys. Acta 510*, 124–129.
Herbette, L., Napolitano, C. A., & McDaniel, R. V. (1984) *Biophys. J. 46*, 677–685.
Heyn, M. P. (1979) *FEBS Lett. 108*, 359–364.
Holowka, D., & Baird, B. (1983a) *Biochemistry 22*, 3466–3474.
Holowka, D., & Baird, B. (1983b) *Biochemistry 22*, 3475–3484.
Huang, C. (1969) *Biochemistry 8*, 344–351.
Huang, C., & Mason, J. T. (1978) *Proc. Natl. Acad. Sci. U.S.A. 75*, 308–310.
Huang, C., Snipe, J. P., Chow, S. T., & Martin, R. B. (1974) *Proc. Natl. Acad. Sci. U.S.A. 71*, 359–362.
Inoko, Y., & Mitsui, T. (1978) *J. Phys. Soc. Jpn. 44*, 1918–1924.
Jabloński, A. (1960) *Bull. Acad. Pol. Sci., Ser. Sci., Math., Astron. Phys. 8*, 259–264.
Jähnig, F. (1979) *Proc. Natl. Acad. Sci. U.S.A. 76*, 6361–6365.
Janiak, M. J., Small, D. M., & Shipley, G. G. (1976) *Biochemistry 15*, 4575–4580.
Janiak, M. J., Small, D. M., & Shipley, G. G. (1979) *J. Biol. Chem. 254*, 6068–6078.
Kawato, S., Kinosita, K., Jr., & Ikegami, A. (1977) *Biochemistry 16*, 2319–2324.
Kawato, S., Kinosita, K., Jr., & Ikegami, A. (1978) *Biochemistry 17*, 5026–5031.
Kinosita, K., Jr., Kawato, S., & Ikegami, A. (1977) *Biophys. J. 20*, 289–305.
Koppel, D. E., Fleming, P. J., & Strittmatter, P. (1979) *Biochemistry 18*, 5450–5457.
Lehrer, S. S. (1971) *Biochemistry 10*, 3254–3263.
Levine, Y. K., & Wilkins, M. H. F. (1971) *Nature (London), New Biol. 230*, 69–72.
Levine, Y. K., Bailey, A. I., & Wilkins, M. H. F. (1968) *Nature (London) 220*, 577–578.
Lewis, B. A., & Engelman, D. M. (1983) *J. Mol. Biol. 166*, 211–217.
Lis, L. J., McAlister, M., Fuller, N., Rand, R. P., & Parsegian, V. A. (1982) *Biophys. J. 37*, 657–666.
Martin, M. M. (1975) *Chem. Phys. Lett. 35*, 105–111.
McClare, C. W. F. (1971) *Anal. Biochem. 39*, 527–530.
Moore, S., & Stein, W. H. (1948) *J. Biol. Chem. 176*, 367–388.
Newman, G. C., & Huang, C.-H. (1975) *Biochemistry 14*, 3363–3370.
Ohki, K., Nozawa, Y., & Ohnishi, S. I. (1979) *Biochim. Biophys. Acta 554*, 39–50.
Parker, C. A., & Rees, W. T. (1960) *Analyst (London) 85*, 587–600.
Parsegian, V. A., Fuller, N., & Rand, R. P. (1979) *Proc. Natl. Acad. Sci. U.S.A. 76*, 2750–2754.
Perrin, F. (1929) *Ann. Phys. (Paris) 12*, 169–275.
Rand, R. P., Parsegian, V. A., Henry, J. A. C., Lis, L. J., & McAlister, M. (1980) *Can. J. Biochem. 58*, 959–968.
Rigaud, J.-L., Gary-Bobo, C. M., & Lange, Y. (1972) *Biochim. Biophys. Acta 266*, 72–84.
Seelig, J., & Seelig, A. (1980) *Q. Rev. Biophys. 13*, 19–68.
Shimshick, E. J., & McConnell, H. M. (1973) *Biochem. Biophys. Res. Commun. 53*, 446–451.
Shinitzky, M., & Barenholz, Y. (1974) *J. Biol. Chem. 249*, 2652–2657.
Shinitzky, M., & Barenholz, Y. (1978) *Biochim. Biophys. Acta 515*, 367–394.
Shinitzky, M., & Yuli, I. (1982) *Chem. Phys. Lipids 30*, 261–282.
Singer, S. J., & Nicolson, G. L. (1972) *Science (Washington, D.C.) 175*, 720–731.
Sloane-Stanley, G. H. (1967) *Biochem. J. 104*, 293–295.
Spencer, R. D., & Weber, G. (1970) *J. Chem. Phys. 52*, 1654–1663.
Struck, D. K., & Pagano, R. E. (1980) *J. Biol. Chem. 255*, 5404–5410.
Stryer, L. (1978) *Annu. Rev. Biochem. 47*, 819–846.
Stubbs, G. W., Litman, B. J., & Barenholz, Y. (1976) *Biochemistry 15*, 2766–2772.
Thomas, D. D., Carlsen, W. F., & Stryer, L. (1978) *Proc. Natl. Acad. Sci. U.S.A. 75*, 5746–5750.
Thulborn, K. R. (1981) in *Fluorescent Probes* (Beddard, G. S., & West, M. A., Eds.) pp 113–139, Academic Press, New York.
Thulborn, K. R., & Sawyer, W. H. (1978) *Biochim. Biophys. Acta 511*, 125–140.
Tilley, L. M., Thulborn, K. R., & Sawyer, W. H. (1979) *J. Biol. Chem. 254*, 2592–2594.
Tweet, A. G., Bellamy, W. D., & Gaines, G. L., Jr. (1964) *J. Chem. Phys. 41*, 2068–2077.
Ware, W. R., & Rothman, W. (1976) *Chem. Phys. Lett. 39*, 449–453.
Weber, G., & Teale, F. W. J. (1957) *Trans. Faraday Soc. 53*, 646–655.
Wharton, S. A., de Martinez, S. S. G., & Green, C. (1980) *Biochem. J. 191*, 785–790.
Wilkins, M. H. F., Blaurock, A. E., & Engelman, D. M. (1971) *Nature (London), New Biol. 230*, 72–76.
Wolber, P. K., & Hudson, B. S. (1979) *Biophys. J. 28*, 197–210.
Yguerabide, J. (1968) *Rev. Sci. Instrum. 39*, 1048–1052.
Zannoni, C., Arcioni, A., & Cavatorta, P. (1983) *Chem. Phys. Lipids 32*, 179–250.